MRE11–RAD50–NBS1 is a critical regulator of FANCD2 stability and function during DNA double-strand break repair

Céline Roques, Yan Coulombe, Mathieu Delannoy, Julien Vignard, Simona Grossi, Isabelle Brodeur, Amélie Rodrigue, Jean Gautier, Alicja Z Stasiak, Andrzej Stasiak, et al.

The EMBO Journal (2009) 28, 2400–2413 | © 2009 European Molecular Biology Organization | All Rights Reserved 0261-4189/09
www.embojournal.org

THE EMBO JOURNAL

MRE11–RAD50–NBS1 is a critical regulator of FANCD2 stability and function during DNA double-strand break repair

Céline Roques[1], Yan Coulombe[1], Mathieu Delannoy[2], Julien Vignard[1], Simona Grossi[2], Isabelle Brodeur[1], Amélie Rodrigue[1], Jean Gautier[3], Alicja Z Stasiak[4], Andrzej Stasiak[4], Angelos Constantinou[2] and Jean-Yves Masson[1,*]

[1]Genome Stability Laboratory, Laval University Cancer Research Center, Hôtel-Dieu de Québec, Québec, Canada, [2]Department of Biochemistry, University of Lausanne, BIL Biomedical Research Center, Lausanne, Switzerland, [3]Columbia University, Institute for Cancer Genetics, Irving Cancer Research Center, New York, NY, USA and [4]Center for Integrative Genomics, Faculty of Biology and Medicine, University of Lausanne, Lausanne, Switzerland

Monoubiquitination of the Fanconi anaemia protein FANCD2 is a key event leading to repair of interstrand cross-links. It was reported earlier that FANCD2 co-localizes with NBS1. However, the functional connection between FANCD2 and MRE11 is poorly understood. In this study, we show that inhibition of MRE11, NBS1 or RAD50 leads to a destabilization of FANCD2. FANCD2 accumulated from mid-S to G2 phase within sites containing single-stranded DNA (ssDNA) intermediates, or at sites of DNA damage, such as those created by restriction endonucleases and laser irradiation. Purified FANCD2, a ring-like particle by electron microscopy, preferentially bound ssDNA over various DNA substrates. Inhibition of MRE11 nuclease activity by Mirin decreased the number of FANCD2 foci formed *in vivo*. We propose that FANCD2 binds to ssDNA arising from MRE11-processed DNA double-strand breaks. Our data establish MRN as a crucial regulator of FANCD2 stability and function in the DNA damage response.

The EMBO Journal (2009) **28,** 2400–2413. doi:10.1038/emboj.2009.193; Published online 16 July 2009
Subject Categories: genome stability & dynamics
Keywords: DNA metabolism; Fanconi anaemia; homologous recombination; Mirin

Introduction

Fanconi anaemia (FA) is a rare autosomal recessive disease characterized by congenital malformations, severe bone marrow failure and cancer predisposition (Grompe and D'Andrea, 2001). FA is an inherited cancer susceptibility disorder resulting from germline disruption of one of the thirteen FA genes. FA-deficient cell lines exhibit a spontaneous chromosomal instability and quadriradial chromosomes. The FA pathway consists of an FA core complex of at least 10 subunits (FANCA, B, C, E, F, G, L, M, FAAP100 and FAAP24) (Wang, 2007), FANCD2 (Garcia-Higuera *et al*, 2001; Timmers *et al*, 2001) and FANCI (Gurtan *et al*, 2006; Sims *et al*, 2007; Smogorzewska *et al*, 2007). Moreover, other FA proteins closely related to the breast/ovarian cancer susceptibility genes products, BRCA1 and BRCA2, and associated proteins were identified. FANCD1 is identical to BRCA2 (Howlett *et al*, 2002), whereas FANCN is also known as PALB2 (partner and localizer of BRCA2) (Reid *et al*, 2007; Xia *et al*, 2007). FANCJ (BACH1/BRIP1) is a DNA helicase that interacts directly with BRCA1 (Bridge *et al*, 2005; Levitus *et al*, 2005).

It is believed that cellular resistance to DNA cross-linking agents requires all FA proteins. DNA damage activates the FA core complex to monoubiquitinate FANCD2 and also FANCI (Gurtan *et al*, 2006; Sims *et al*, 2007; Smogorzewska *et al*, 2007). FANCL is most likely the E3 ligase responsible for FANCD2 monoubiquitination (Meetei *et al*, 2004). FANCD2 monoubiquitination occurs during S-phase progression (Taniguchi *et al*, 2002a). Factors that interfere with the normal DNA replication process such as the DNA cross-linking agent mitomycin C (MMC), hydroxyurea, UVC or rereplication events are all potent inducers of the monoubiquitination of FANCD2 (Garcia-Higuera *et al*, 2001; Pichierri and Rosselli, 2004; Zhu and Dutta, 2006). FA-deficient cells are notably hypersensitive to interstrand-DNA and protein-DNA cross-linking agents, whereas FANCD2 is activated by a variety of replication stresses (Auerbach and Wolman, 1976; Ridpath *et al*, 2007). DNA interstrand cross-links (ICLs) represent a unique challenge for the repair machineries because covalent modifications that link two DNA strands preclude simple excision/repair synthesis mechanisms. Several pieces of evidence suggest that the repair of ICLs in mammalian cells occurs mainly during DNA replication, features DNA double-strand breaks (DSBs) as repair intermediates and requires the homologous recombination machinery (Akkari *et al*, 2000; De Silva *et al*, 2000; Godthelp *et al*, 2002). Replication-coupled repair of ICLs occurs when two replication forks converge at the ICL (Raschle *et al*, 2008). During ICL repair, FA proteins are thought to orchestrate the coordinated action of nucleases, translesion DNA polymerases and the homologous recombination machinery to produce intact daughter duplexes (Niedernhofer *et al*, 2005).

The MRN (MRE11–RAD50–NSB1) complex is a central player in checkpoint signalling of DNA damage, DNA repair and telomere maintenance (Dery and Masson, 2007; Williams *et al*, 2007). MRE11 has a 3′–5′ Mn^{2+}-dependent exonuclease activity on DNA substrates with blunt or 5′ protruding

*Corresponding author. Laval University Cancer Research Center, Hôtel-Dieu de Québec, 9 McMahon, Québec, PQ, Canada G1R 2J6. Tel.: +1 418 525 4444 Ext. 15154; Fax: +1 418 691 5439; E-mail: Jean-Yves.Masson@crhdq.ulaval.ca

Received: 15 January 2009; accepted: 17 June 2009; published online: 16 July 2009

ends. MRE11 displays endonuclease activity on hairpin and single-stranded DNA (ssDNA) substrates (Paull and Gellert, 1998; Trujillo *et al*, 1998). RAD50 is related to the structural maintenance of chromosome proteins. Using its long coiled coils, it can bridge DNA ends together, therefore, facilitating DNA end processing (Moreno-Herrero *et al*, 2005). NBS1, which has key functions in the DNA damage response pathway (Lim *et al*, 2000) is a nuclear protein with an N-terminal forkhead-associated (FHA) domain, a breast cancer BRCA1 C-terminal (BRCT) domain and a second BRCT domain (termed BRCT2) (Becker *et al*, 2006).

Several evidences implicate the budding yeast and human MRN complex in ICL repair. Disruption of *Saccharomyces cerevisiae* MRE11 leads to sensitivity to nitrogen mustard (McHugh *et al*, 2000). Inhibition of all the constituents of the MRN complex, using RNA interference against MRE11 (Pichierri and Rosselli, 2004), RNA antisense-mediated reduction of RAD50 (Kim *et al*, 2002) or NBS1 (Nakanishi *et al*, 2002), leads to sensitivity to MMC. However, it is not clear whether this sensitivity is related to a defect in the FA pathway. It has been reported that FANCD2 interacts with NBS1. Moreover, MRE11 and FANCD2 co-localize during S phase and after ionizing radiation treatment (Nakanishi *et al*, 2002). In addition, subnuclear assembly of MRN depends on the FANCC protein (Pichierri *et al*, 2002). However, the control of FA proteins by MRE11–RAD50–NBS1 remains elusive. In this manuscript, we investigate the interplay between MRN and FANCD2 and show that these proteins are functionally connected in many ways. We show that MRN interacts and co-purifies with FANCD2, regulates FANCD2 stability and controls FANCD2 localization to DNA damage sites.

Results

FANCD2 stability is dependent on MRE11, RAD50 and NBS1

It was earlier reported that MRE11 and FANCD2 co-localize during S-phase, and after ionizing radiation treatment (Nakanishi *et al*, 2002) and MRE11 localization to a unique I-SceI, DSB is modulated by arginine methylation (Dery *et al*, 2008). Therefore, we tested whether the co-localization of FANCD2 and MRE11 was affected by arginine methylation in the same experimental setting. We followed the formation of a single and defined FANCD2 focus by immunofluorescence on expression of I-SceI. Interestingly, FANCD2 localization to the unique DSB was abrogated in cells treated with the methylation inhibitor ADOX, whereas γ-H2AX remained unaffected (Figure 1A). FACS analysis revealed that ADOX-treated cells, although growing slower, were not blocked in a specific phase of the cell cycle suggesting that γ-H2AX abrogation was not due to a cell cycle effect (Figure 1B).

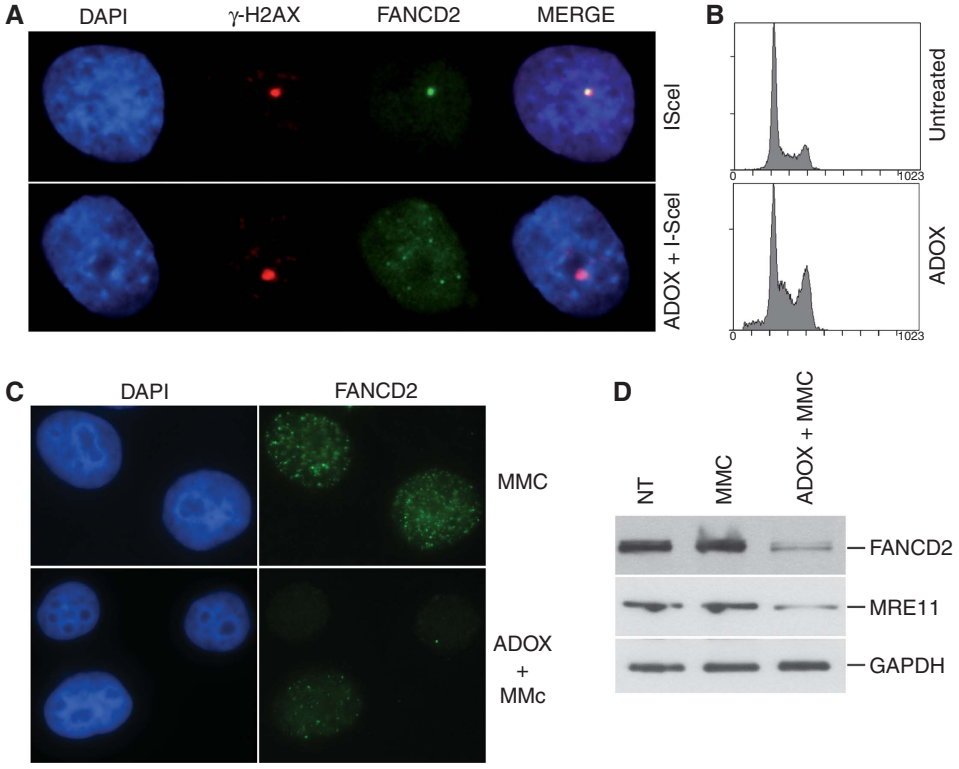

Figure 1 (**A**) The localization of FANCD2 to a unique DSB *in vivo* is dependent on arginine methylation. Top: γ-H2AX and FANCD2 foci formation on a unique DSB *in vivo*. DR95 cells were transfected with pCBASce (encoding I-SceI) and immunofluorescence was conducted with the indicated antibodies. Micrographs depict DNA stained with DAPI (blue); anti-γ-H2AX (red); anti-FANCD2 (green). The merge picture is an overlay of the green, red, and blue channels. Bottom: the same experiment was performed with cells treated with the arginine methylation inhibitor ADOX. (**B**) FACS analysis of mock-treated Hela cells or treated with ADOX (250 μM) for 24 h. (**C**) MMC-inducible FANCD2 foci formation is reduced in the presence of ADOX. Hela cells were treated with MMC (2 μM/1 h) or ADOX (250 μM) for 24 h followed by MMC treatment (2 μM/1 h). Immunofluorescence studies were performed with anti-FANCD2 (green). (**D**) Lack of arginine methylation destabilizes FANCD2. DR95 cells were mock treated (NT), treated with MMC (600 nM/1 h) or ADOX (250 μM) for 24 h followed by MMC treatment (600 nM/1 h) and western blotting with FANCD2, MRE11 and GAPDH antibodies as indicated.

Next, we assessed whether MMC-dependent FANCD2 foci formation was diminished in the presence of ADOX (Figure 1C). Likewise, ADOX reduced the recruitment of FANCD2 to DNA damage sites caused by MMC. Interestingly, we observed that addition of ADOX leads to a decrease in MRE11 and FANCD2 expression, whereas GAPDH protein levels were constant (Figure 1D).

Given the decrease in MRE11 level after ADOX treatment (Figure 1D, 250 μM/24 h), we reasoned that FANCD2 destabilization could be caused by MRE11 inhibition rather than the loss of arginine methylation. To test this, cells were treated with small interfering RNA (siRNA) against FANCD2 (Figure 2A), NBS1 (Figure 2B), MRE11 (Figure 2C) and RAD50 (Figure 2E). siRNA against FANCD2 led to a decrease of the soluble pool of FANCD2 after 24 h without affecting MRE11, RAD50 or NBS1 levels (Figure 2A). In contrast, by 48 h, inhibition of NBS1 led to a decrease in FANCD2 (Figure 2B). Likewise, siRNA against MRE11 led to a concomitant decrease of FANCD2, MRE11, RAD50 and NBS1 by 48 h (Figure 2C). As a control, the FANCI protein levels

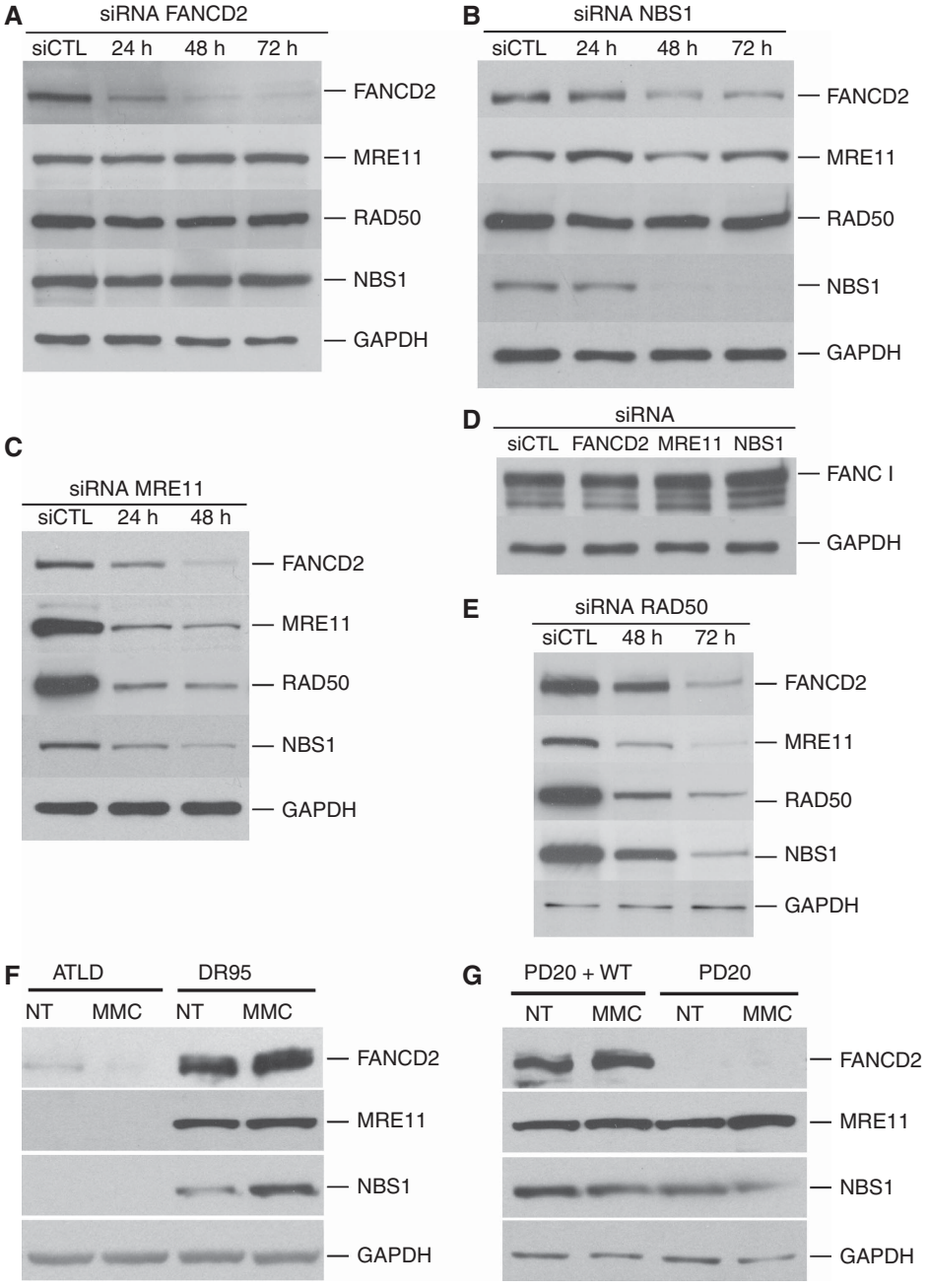

Figure 2 Destabilization of FANCD2 after siRNA inhibition of MRE11, NBS1 or RAD50. Whole-cell extracts from siCTL transfected or Hela cells transfected with siRNA against FANCD2 (**A**), NBS1 (**B**) and MRE11 (**C**) were subjected to western blotting with FANCD2, MRE11, RAD50, NBS1 and GAPDH antibodies. (**D**) FANCI is not destabilized in mock-transfected, FANCD2, MRE11 or NBS1 knockdowns. (**E**) Whole-cell extracts from siCTL transfected or Hela cells transfected with siRNA against RAD50 were subjected to western blotting with FANCD2, MRE11, RAD50, NBS1 and GAPDH antibodies. (**F**, **G**) ATLD cells have low levels of FANCD2, whereas DR95 or FANCD2-complemented PD20 cells display normal levels. Cells were either untreated (NT) or treated with MMC (600 nM/1H), whole-cell extracts were prepared and subjected to western blotting, as indicated.

remained unaffected by inhibition of FANCD2, MRE11 or NBS1 (Figure 2D). Consistent with this, inactivation of FANCD2 in DT40 or human cells resulted in loss of FANCI monoubiquitination, but not stability (Sims *et al*, 2007; Ishiai *et al*, 2008). To strengthen the idea that MRN is required for FANCD2 stability, we performed a siRNA knockdown of RAD50. We observed the concomitant reduction of all components of the MRN complex and FANCD2 at 48–72 h after transfection (Figure 2E). As inhibition of any protein of the MRN complex lead to a reduction of FANCD2 protein levels, we inferred that this effect was due to the destabilization of FANCD2 rather than off-targeting of the FANCD2 mRNA by MRN siRNAs. This is supported by microarray analyses, as siRNA against MRE11 did not affect the mRNA levels of FANCD2, NBS1 or RAD50 ($<$1.5-fold) significantly, whereas MRE11 mRNA levels were reduced by 15.7-fold (data not shown). As FANCD2, NBS1 and MRE11 protein levels are relatively stable during the cell cycle (Supplementary Figure 1A), the destabilization is not cell cycle dependent.

Extracts from ataxia telangiectasia-like disease (ATLD) cells, carrying a homozygous truncating mutation in *MRE11* gene, have no detectable level of MRE11 protein and very low levels of both NBS1 and RAD50 proteins as reported earlier (Stewart *et al*, 1999). We, therefore, monitored the levels of FANCD2 in ATLD cells. Strikingly, FANCD2 protein levels were severely reduced in control and MMC-treated cells (Figure 2F). In contrast, the levels of FANCD2 and MRE11 were unchanged in MRE11-proficient cells such as DR95, or complemented FANCD2-deficient PD20 cells, which express FANCD2 at normal levels (Figure 2F and G). Consistent with a decrease in FANCD2 levels in MRE11-deficient cells, siRNA against MRE11 and NBS1 also led to a decrease of FANCD2 foci in untreated and DNA-damaged cells (Figure 3A, quantification is provided in Supplementary Figure 1B).

Stabilization of one protein by a partner often involves specific protein–protein interactions. To assess whether MRN and FANCD2 could form a complex, we performed gel filtration analysis, co-immunoprecipitation of endogenous proteins, co-purification of MRN–FANCD2 complexes and co-immunoprecipitation of purified proteins. First, gel filtration analysis of FANCD2-complemented PD20 cells extracts revealed that the MRN complex eluted in fractions 13–18 along with the bulk of FANCD2 (Figure 3B). Similar results were also obtained with Hela nuclear extracts (data not shown). Second, we examined the ability of the MRN complex to associate with FANCD2 in an heterologous system. Using baculovirus-infected Sf9 cells, we observed a direct interaction between FANCD2, NBS1 and MRE11 (Supplementary Figure 2A). Third, these interactions were confirmed by reciprocal co-immunoprecipitation of endogenous FANCD2 and MRN from human PD20-complemented cell extracts (Figure 3C). Fourth, we performed the co-purification of MRE11-His_6, RAD50-His_6 and NBS1 (Lee and Paull, 2006) with FANCD2-Flag. Control experiments showed that FANCD2-Flag could not bind to nickel agarose on its own (Supplementary Figure 2B). Sf9 extracts expressing MRE11-His_6, RAD50-His_6, NBS1 and FANCD2-Flag were fractionated through nickel agarose to bind the His-tagged MRE11 and RAD50 proteins, and the eluted fractions (F4-F5-F6, $\sim$125 mM imidazole) were subjected to Q-sepharose ion exchange. Although devoided of an histidine tag, FANCD2 co-eluted with MRN on nickel agarose and also Q-sepharose ($\sim$400 mM KCl) (Figure 3D). Fifth, a complex between purified MRN and FANCD2 was detected by immunoprecipitation analysis (Figure 3E). Collectively, these data suggest an *in vivo* and *in vitro* interaction between the MRN and FANCD2 proteins.

FANCD2 associates with ssDNA in vivo

Next, we sought to address the functional consequences of these interactions. We hypothesized that, besides stabilization, the relationship between FANCD2 and MRN might extend to the functional level. We observed that FANCD2 co-localized with MRE11, RPA and γ-H2AX after laser-induced DNA DSBs by immunofluorescence staining (Figure 4A). The nuclease activity of MRE11 is required for the processing of DNA DSBs into ssDNA tails, which are bound by the replication protein A and then trigger the DNA damage response in S phase (Jazayeri *et al*, 2006). To test whether FANCD2 co-localizes with ssDNA formed during DNA replication, we used a method that is based on the selective detection of BrdU by anti-BrdU antibodies when the substituted DNA is in an ssDNA form (Raderschall *et al*, 1999). RV-A, a FA group A cell line complemented with a recombinant retrovirus encoding FANCA, were uniformly labelled with BrdU, and then stained with anti-BrdU antibodies, under native conditions. To induce the formation of a significant amount of microscopically visible ssDNA foci (compatible with co-localization studies), RV-A cells were both synchronized with HU and then exposed to MMC (0.1 μg/ml), during the last hour of the replication block. We evaluated the proportion of ssDNA foci that overlapped with RPA, with the strand exchange protein RAD51 or with FANCD2: 88 and 67% of ssDNA foci co-localized with RPA and RAD51 foci, respectively, indicating that BrdU staining in native conditions represents genuine ssDNA (Figure 4B). Likewise, 81% of ssDNA foci co-localized with FANCD2. We also localized replication factories, FANCD2 and ssDNA foci simultaneously. Figure 4C shows a nucleus with FANCD2 and ssDNA signals overlapping in the nuclear interior in the presence of DNA replication ongoing at the nuclear periphery. Hence, FANCD2 foci are located at nuclear sites enriched in ssDNA that are distinct from nuclear regions engaged in DNA replication. We also tested whether increased ssDNA accessibility or DNA damage, through inhibition of RPA, resulted in an accumulation of FANCD2. siRNA directed against RPA (Figure 4D) led to an increase in FANCD2 foci formation in the absence of exogenous DNA damage (Figure 4E and F). Statistical analysis of the data distribution gave a χ^2 *P*-value <0.001.

Purified FANCD2 binds DNA

Our data suggest that FANCD2 associates with damage-induced ssDNA in S phase. Thus, we verified whether FANCD2 exhibits affinity for ssDNA *in vitro*. First, we generated a baculovirus expressing FANCD2 Strep- and His tagged at the N- and C-termini, respectively. FANDC2 was purified using a double-affinity tag purification using metal and Streptactin-affinity chromatography. This strategy yielded full-length FANCD2 purified to homogeneity and free of degradation products (Figure 5A). We compared the affinity of FANCD2 for ssDNA and double-stranded DNA (dsDNA)

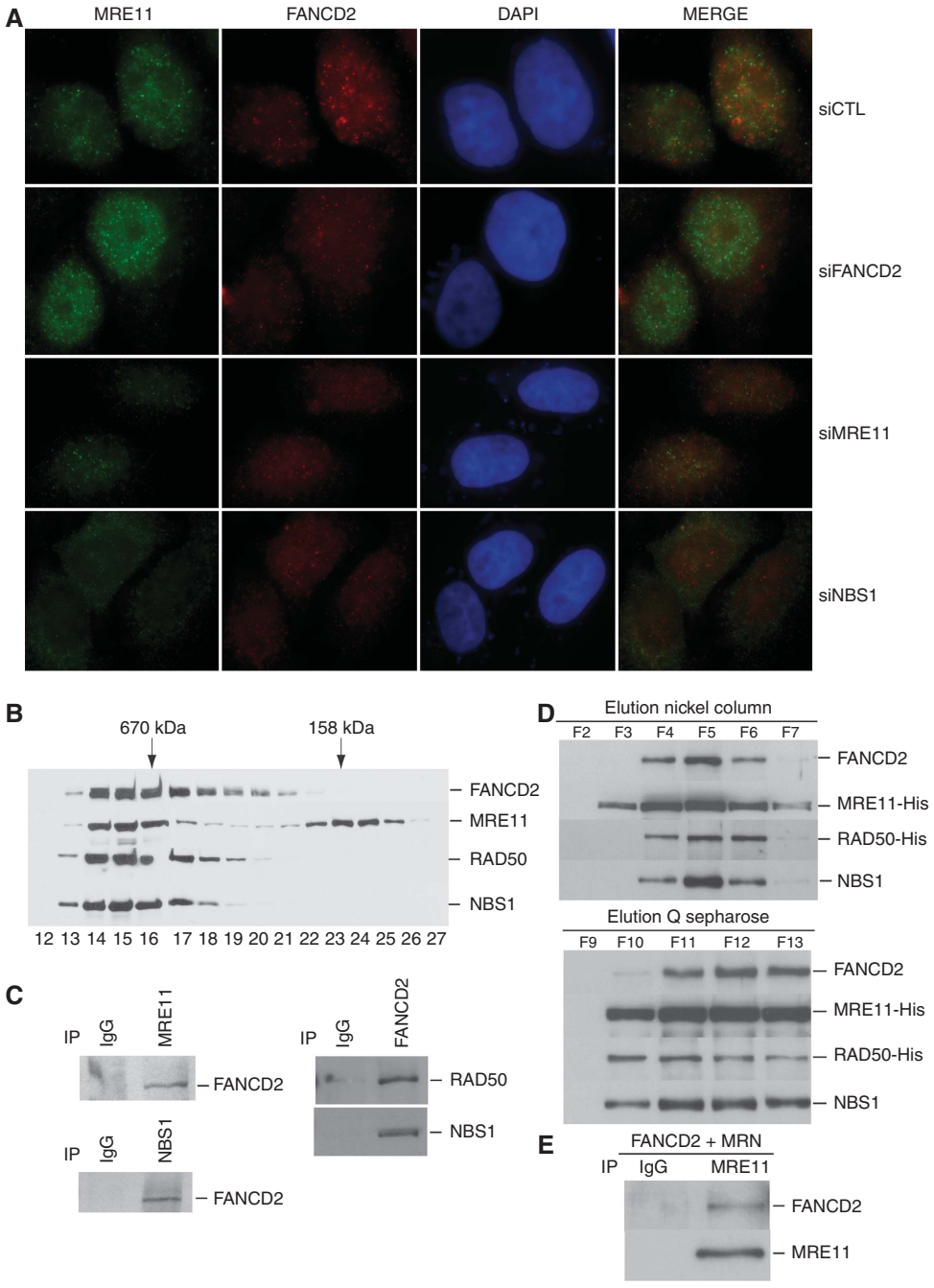

Figure 3 (**A**) siMRE11 and siNBS1 impair FANCD2 foci formation. DR95 cells were transfected with the indicated siRNAs followed by immunofluorescence analysis with the indicated antibodies. Micrographs depict anti-MRE11 (green); anti-FANCD2 (red); DNA stained with DAPI (blue). The merge picture is an overlay of the green and red channel. (**B**) FANCD2 and MRN co-elute by gel filtration analysis of whole-cell extracts of FANCD2-complemented PD20 cells through Superdex 200. Top part: size standards, bottom part: western blotting of the fractions using anti-FANCD2, anti-MRE11, anti-RAD50 and anti-NBS1, respectively. (**C**) Endogenous FANCD2 interacts with the MRN complex in human FANCD2-complemented PD20 cells. Immunoprecipitations were conducted with IgG alone or polyclonal antibodies against FANCD2, MRE11, NBS1 and blotted against FANCD2, RAD50 or NBS1 as indicated. (**D**) Co-elution of FANCD2, MRE11, RAD50 and NBS1. Sf9 cells were infected with the indicated baculoviruses and extracts were loaded onto a Nickel column to bind the His-tagged proteins (MRE11 and RAD50) and associated proteins. Fractions 4, 5, 6 and 7 were pooled together, dialysed and loaded on a Q-sepharose column. The interacting proteins were eluted and identified by western blotting using the indicated antibodies. Eluting fractions are indicated. (**E**) Co-immunoprecipitation of purified Strep-FANCD2-His and MRN. Immunoprecipitations were conducted with IgG alone or a polyclonal antibody against MRE11 and blotted against FANCD2 and MRE11 as indicated.

(100-mer oligonucleotides and 100 bp duplex DNA) as well as splayed arms and Holliday junction substrates by gel retardation assays. FANCD2 bound all substrates, but displayed higher affinity for ssDNA than dsDNA (at 50 nM, 43.5% of ssDNA was bound compared with 8.4% for dsDNA). FANCD2 bound ssDNA with higher affinity than splayed arms (31.6% at 50 nM) or Holliday junctions (21.4% at 50 nM) (Figure 5B and C). The formation of protein–DNA complexes on ssDNA was optimal at 50 mM NaCl and occurred at concentrations of $Mg(CH_3COO)_2$ ranging

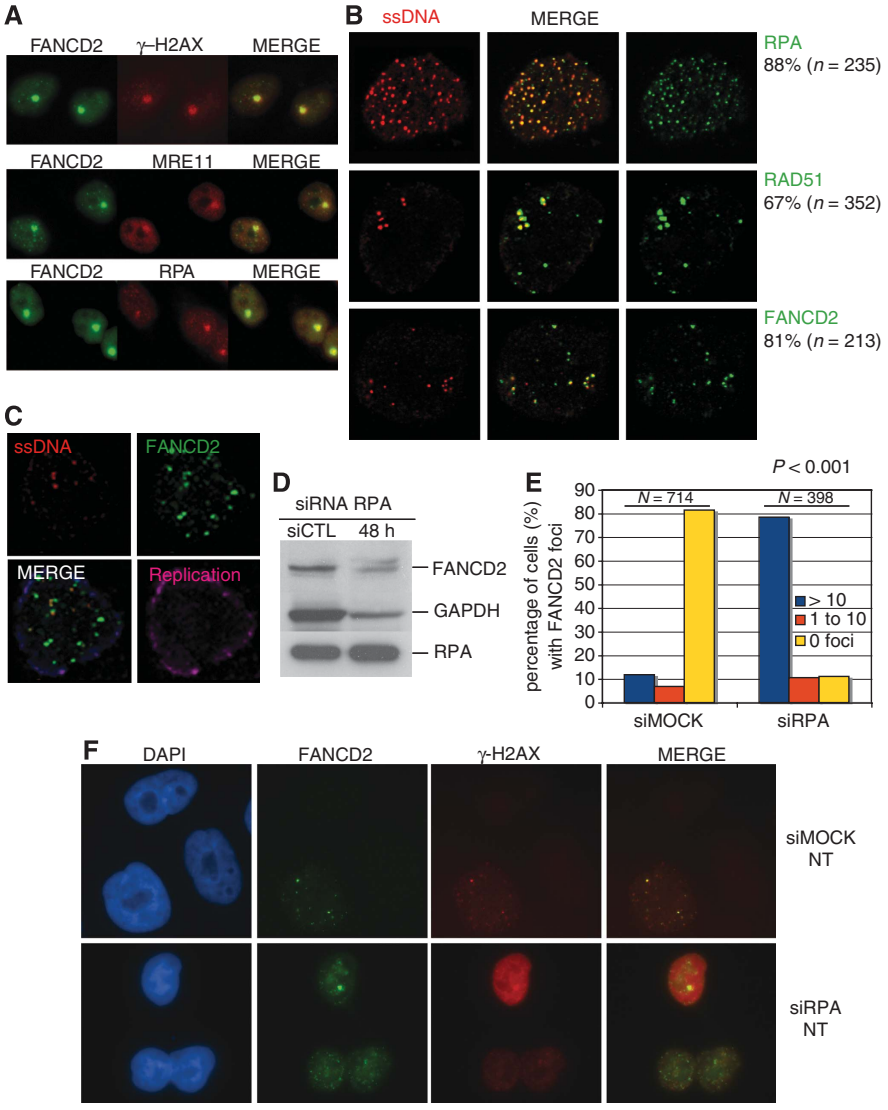

Figure 4 (**A**) FANCD2 (green) co-localizes with γ-H2AX, MRE11 and RPA (red) at laser-induced DSBs in Hela cells. The merge picture is an overlay of the green and red channels. (**B**) Co-localization of ssDNA foci with RPA, RAD51 and FANCD2. Cells were incubated for 12 h with hydroxyurea, and 0.1 mg/ml of MMC was added during the last hour in HU. The ssDNA foci (red fluorescence) were revealed as described in Material and methods, 9 h after release from the G1/S block. Nuclei were counterstained with anti-RPA, anti-RAD51 and anti-FANCD2 antibodies (green fluorescence) as indicated. Yellow foci in merged images are indicative of co-localization. The percentage of ssDNA foci co-localizing with RPA, RAD51 and FANCD2 is indicated (*n* is the number of ssDNA foci analysed) and counted as follows. RPA + ssDNA: 56 cells were analysed, 207 ssDNA foci co-localize with RPA, 28 ssDNA foci without RPA. Total foci: 235, 88% co-localization. RAD51 + ssDNA: 101 cells analysed, 235 ssDNA foci co-localize with RAD51, 117 ssDNA foci without RAD51. Total foci 352, 67% co-localization. FANCD2 + ssDNA: 103 cells analysed, 172 ssDNA foci co-localize with FANCD2 foci, 41 ssDNA foci without FANCD2. Total foci 213, 81% co-localization. (**C**) FANCD2 foci are located at sites of ssDNA accumulation that are distinct from nuclear regions engaged in DNA replication. Cells were uniformly labelled with CldU and pulse labelled with IdU, 9 h after release in S phase. One representative nucleus is shown; ssDNA foci were stained with anti-CldU antibody (red fluorescence), and FANCD2 foci with anti-FANCD2 antibody (green fluorescence). Antigen–antibody complexes were fixed and then the preparations were denatured to reveal replication factories with anti-IdU antibody (magenta staining) as described in Material and methods. (D–F) siRNA against RPA induces FANCD2 foci formation without affecting its stability. (**D**) Whole-cell extracts from siCTL transfected or Hela cells transfected with siRNA against RPA were subjected to western blotting with FANCD2, RPA and GAPDH antibodies. (**E**) Foci counts data were analysed using the χ^2 test with R version 2.7.2 (http://www.r-project.org/). The resulting contingency table is displayed as an histogram. Foci distributions are considered as significantly different with a *P*-value lower than 0.01. The percentage of cells displaying no nuclear foci (blue), 0–10 foci (red) or more that 10 foci (yellow) is depicted. (**F**) Hela cells were transfected with the indicated siRNAs followed by immunofluorescence analysis with anti-FANCD2 (green) or anti-γ-H2AX. DNA stained with DAPI (blue). The merge picture is an overlay of the green and red channel.

from 1 to 10 mM, with an optimal concentration at 2 mM. Protein–DNA complexes gradually disassembled at increasing concentrations of KCl over 150 mM (data not shown). Binding to ssDNA was observed both in the absence of ATP or ATP analogues, suggesting that DNA binding could occur without ATP or ATP hydrolysis. Preincubation of FANCD2 with FANCD2 polyclonal antibody before nucleic acid addition abrogated DNA binding, suggesting that the DNA-binding activity is FANCD2 dependent (Supplementary Figure 2C).

We further explored the association of FANCD2 with DNA using circular ∅X174 ssDNA (5386 nt) and linear ∅X174

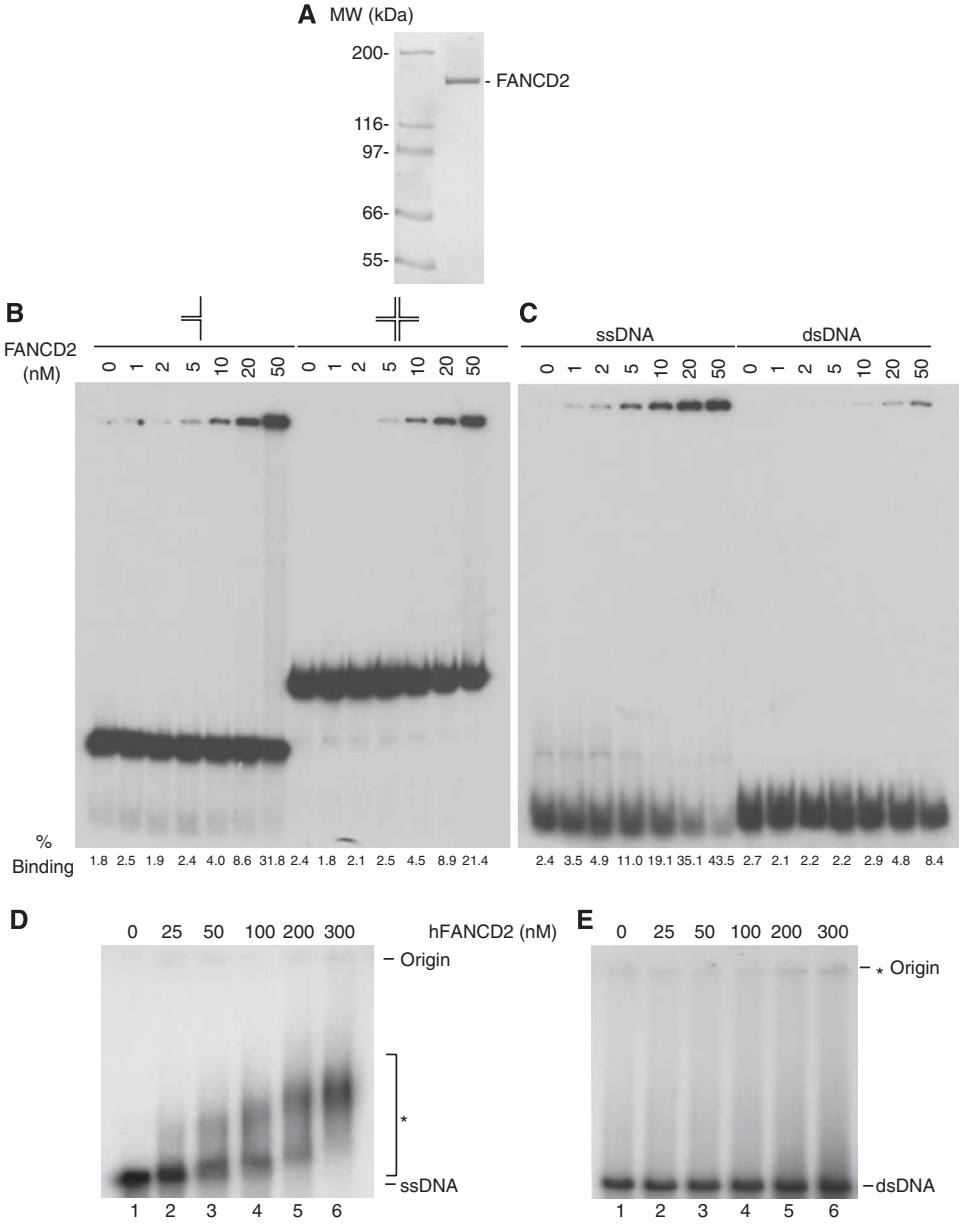

Figure 5 FANCD2 binds ssDNA preferentially. (**A**) SDS–PAGE of the purified human FANCD2 protein. Lane a, MARK12 molecular weight markers; lane b, purified FANCD2 (1 μg). (**B**) The indicated concentration of FANCD2 was incubated with a 5′-^{32}P-labelled flap oligonucleotide or Holliday junction. The percentage of binding is indicated below the gel. (**C**) The indicated concentration of FANCD2 was incubated with a 5′-^{32}P-single-strand oligonucleotide or double-strand oligonucleotide. The percentage of binding is indicated below the gel. Protein–DNA complexes were analysed by PAGE (6%) and visualized by autoradiography. (**D**, **E**) FANCD2 was incubated with 3 μM single-stranded ∅X174 DNA (D) or 6 μM duplex ∅X174 DNA (E), and complexes were analysed by agarose gel electrophoresis. FANCD2–DNA complexes are indicated with an asterisk.

dsDNA (5386 bp). Human FANCD2 displayed non-cooperative binding to ∅X174 ssDNA, as seen by the formation of complexes that exhibited progressively reduced mobility (Figure 5D, lanes 3–6). FANCD2 associated to linear double-stranded ∅X174 with lower affinity than to single-stranded ∅X174 DNA. At the highest protein concentrations, a limited amount of protein–dsDNA networks at the origin of the agarose gel was observed (Figure 5E, compare lanes 4 and 5 with lane 6). In summary, the usage of oligonucleotide-based DNA substrates and plasmid-length DNA molecules led us to the same conclusion: FANCD2 binds ssDNA preferentially compared with dsDNA.

Visualization of FANCD2–DNA complexes by electron microscopy

To visualize FANCD2–∅X174 complexes by electron microscopy, samples were negatively stained with uranyl acetate without fixation. Isolated FANCD2 particles were seen as 10 nM ring-like structures (Figure 6A). A distinct hole was visible at the centre of the particle. Small protein aggregates were also frequently observed in our preparation (Figure 6A). We produced circular-gapped DNA to visualize the interaction of FANCD2 with molecules that comprise both ssDNA and dsDNA regions. Human FANCD2 formed individual clusters of proteins on circular plasmid DNA molecules that

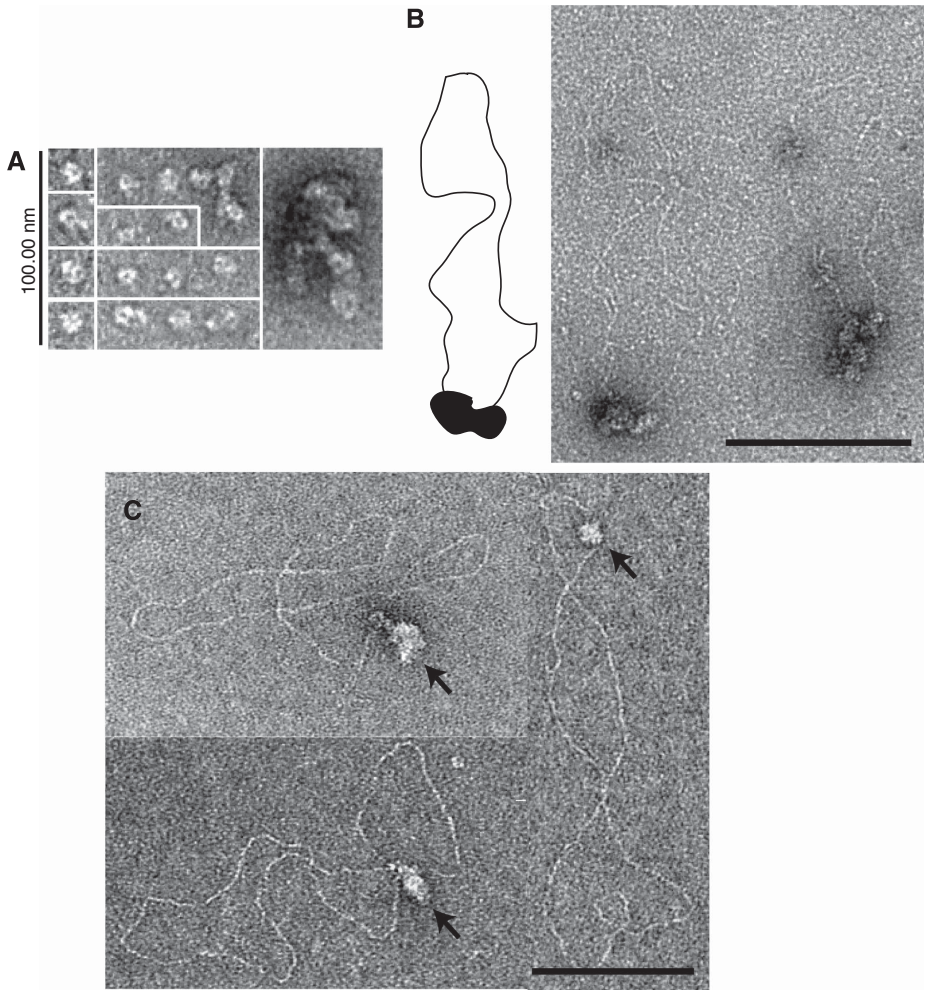

Figure 6 Electron microscopic visualization of FANCD2 and its complexes with ssDNA. (**A**) Visualization of FANCD2 by negative staining in the absence of DNA. FANCD2 was diluted to 100 nM in buffer B before spreading. Monomer-sized particles and small aggregates are shown. A hollow was visible at the centre of the protein. (**B**) Electron microscopic visualization of complexes made by FANCD2 (10 nM) on gapped DNA molecules (603 nucleotides gap). Localized FANCD2 aggregates were observed on the gap DNA substrate. A drawing representing the FANCD2-gap DNA complex is shown. (**C**) Electron microscopic visualization of complexes made by FANCD2 (50 nM) on gapped DNA molecules (40 nucleotides gap). Binding of FANCD2 to the gap is indicated with a black arrow. The magnification bar represents 100 nm.

were otherwise protein free (Figure 6B). As the gapped DNA substrate bears only one ssDNA region (603 nucleotides), and we never observed two separate protein blobs on the molecules, we infer that FANCD2 associates preferentially with the ssDNA portion of the substrate. Gapped DNA with long single-strand region provides many binding sites for FANCD2. To see more elementary functional association with ssDNA, we also looked at interaction with gapped DNA containing one ssDNA region of 40 nucleotides. FANCD2 specifically bound this region and binding to duplex DNA was not visible (Figure 6C). Taken together, these results show that FANCD2 binds ssDNA preferentially compared with dsDNA.

FANCD2 localization to DSBs is dependent on MRE11 activity

To understand how MRN controls FANCD2 accumulation on ssDNA, we took several approaches. First, biochemical studies revealed that a five-fold molar excess of FANCD2 did not affect MRE11 exonuclease activity (Supplementary Figure 3). However, as both proteins bind ssDNA, it was difficult to test whether FANCD2 could accumulate on ssDNA after MRE11 resection *in vitro*. Hence, we turned our attention to *in vivo* assays and ChIP analyses were performed using the DR95 cell line that bears a modified green fluorescent protein gene in which a I-SceI restriction site has been engineered (Pierce *et al*, 1999). Using this strategy, we observed a modest, but reproducible, enrichment of FANCD2 at 0.3 and 3.1 kb from the break. The enrichment at 0.3 kb from the break correlates with NBS1 localization, whereas the enrichment at 3.1 kb is similar to γ-H2AX (Figure 7A). As MRN could be engaged in resection at 0.3 kb from the break, we tested whether FANCD2 localization on DNA DSBs could be correlated with MRE11 nuclease activity *in vivo*. We monitored the formation of FANCD2 foci after addition of Mirin (*Z*-5-(4-hydroxybenzylidene)-2-imino-1,3-thiazolidin-4-one). Mirin is an inhibitor of the MRE11–RAD50–NBS1 complex as recently revealed by Gautier and co-workers (Dupre *et al*, 2008). Mirin prevents MRN-dependent activation of ATM without affecting its protein kinase activity, and inhibits MRE11-associated exonuclease activity. At a concentration of 100 μM, FANCD2 foci formation was reduced in untreated, or etoposide-treated cells (Figure 7B). The difference in foci distribution was significantly different (Figure 7C, χ^2 *P*-value = 6.13E−10 for DMSO versus DMSO with Mirin and 6.03E−17 for DMSO

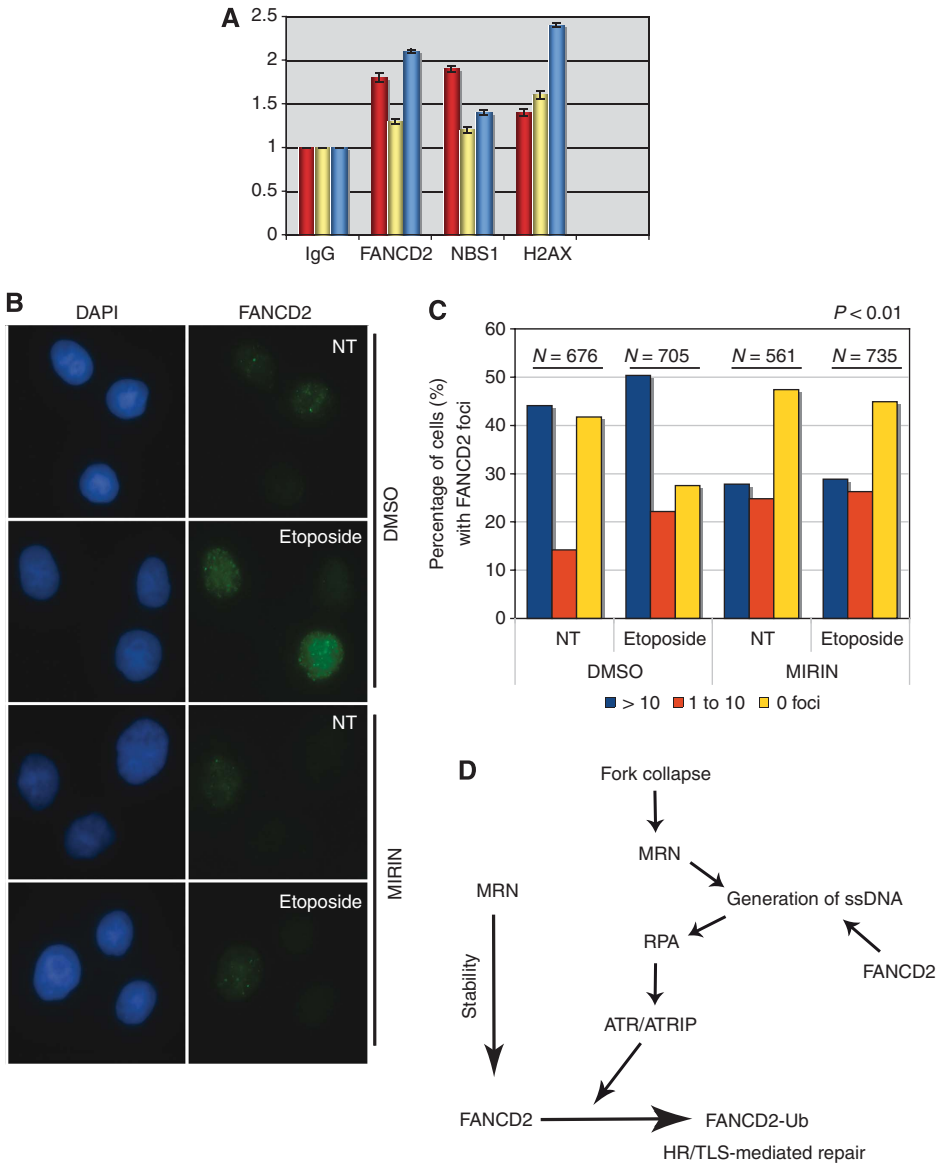

Figure 7 (**A**) Chromatin immunoprecipitations of endogenous FANCD2, NBS1 and γ-H2AX on a unique DSB in DR95 cells. Real-time PCR on ChIP samples were performed at 0.3, 2 and 3.1 kb nucleotides from the break (red, yellow and blue bars, respectively). Fold-enrichment normalized to an endogenous locus is represented. (**B**) Inhibition of MRN by Mirin affects FANCD2 foci formation. Hela cells were pre-treated with DMSO or Mirin (100 μM) and either untreated or treated with etoposide (50 μM, 1 h) and processed for immunofluorescence staining with FANCD2. (**C**) Quantification of FANCD2 foci after inhibition of MRN by Mirin. Hela cells were pre-treated with DMSO (100 μM) or Mirin (100 μM) and either untreated or treated with etoposide (50 μM, 1 h) and processed for immunofluorescence staining with FANCD2. Foci counts data were analysed using the χ^2 test with R version 2.7.2 (http://www.r-project.org/). The resulting contingency table is displayed as an histogram. Foci distributions between groups are considered as significantly different with a *P*-value lower than 0.01. The percentage of cells displaying no nuclear foci (yellow), 0–10 foci (red) or more than 10 foci (blue) is depicted. (**D**) An MRN-dependent pathway regulating FANCD2. Our data suggest two levels of control of FANCD2 by MRN. Left: MRN regulates FANCD2 protein stability. Right: DNA replication of damaged DNA leads to replication fork collapse and DSB formation. MRN resect DSBs to create ssDNA, which is coated by RPA. RPA recruit ATR-ATRIP-HCLK2, FANCM/FAAP24 and the core complex (Collis *et al*, 2008) to promote the monoubiquination of FANCD2 and repair by homologous recombination or translesion synthesis. This process might be facilitated by binding of FANCD2 to ssDNA.

etoposide compared with Mirin etoposide). Collectively, these results suggest that MRN activity is required for FANCD2 localization to DNA damage sites.

Discussion

Removal of DNA ICLs has proven to be a very complicated process because of the involvement of multiple pathways of DNA repair, which include the FA/BRCA pathway, homologous recombination and components of the nucleotide excision and mismatch repair pathways. Owing to this complexity, it is now important to look at the biochemistry and regulation of FA proteins to understand their molecular roles. This study provides valuable information as to the mechanisms by which FANCD2 is regulated during DSB repair.

Interconnection of MRN and FANCD2

An important observation that led us to study the interplay between MRE11 and FANCD2 is the destabilization of FANCD2 protein with siRNA against MRE11, NBS1 or RAD50. Our microarray data suggest that the destabilization

of FANCD2 is not because of an off-target mRNA degradation. The interaction between MRN and FANCD2 seems to be physiologically relevant, as we could purify an MRN–FANCD2 complex from baculovirus-infected Sf9 cells, and we detected an endogenous interaction between MRN and FANCD2 in mammalian cells. However, not all MRN is in complex with FANCD2, as judged by gel filtration analysis. This raises the alternative possibility that D2 stability might be significantly affected by MRN, but not strictly dependent on protein–protein interactions. For instance, the destabilization might also be because of the abolition of an MRN-dependent checkpoint leading to FANCD2 degradation by the proteasome.

Importantly, we are reporting that ATLD cells show low levels of FANCD2. Hence, this serves as a cautionary note when using ATLD cells, as some of the phenotypes attributed to these cells (Stewart *et al*, 1999) might also be related to low levels of FANCD2. For instance, *MRE11*$^{-/-}$ and *NBS*$^{-/-}$ cells display quadriradial chromosome formation, a phenotype that has been considered as a diagnostic of FA (Nakanishi *et al*, 2002). Thus, our findings provide an explanation for these phenotypes.

Unmodified FANCD2 binds DNA

As a first step towards understanding how FANCD2 contributes to DNA maintenance, we developed a new purification procedure yielding highly purified FANCD2. We noticed similarities between FANCD2 and other caretaker proteins involved in DNA repair and/or DNA damage tolerance. Using electron microscopy, the FANCD2 protein was seen as a ring-like particle. These images mostly resemble electron microscopy pictures of monomers of RecT (Thresher *et al*, 1995). RecT is an ~33 kDa protein implicated in the RecE (*recA*-independent) recombination pathway. Unlike FANCD2, however, RecT also forms donut-shaped oligomers and binds ssDNA, but not dsDNA (Hall *et al*, 1993).

It was earlier reported that FANCD2 exhibits preferential affinity for dsDNA ends and four-way junctions, which contain four DNA ends (Park *et al*, 2005). In competition experiments, although supercoiled DNA competed modestly with Holliday junction binding, the most efficient competitor was linear dsDNA containing the most ends. However, the binding to ssDNA was not investigated in this study (Park *et al*, 2005). DNA end binding by FANCD2 may depend on the spontaneous and dynamical opening of duplex DNA (natural DNA breathing). Our results show that FANCD2 has higher affinity for ssDNA over Holliday junctions and dsDNA. Electron microscopic visualization of FANCD2–DNA complexes containing a very short gap of 40 nucleotides confirmed the specificity to ssDNA over dsDNA. Further support for ssDNA binding in an *in vivo* situation, was provided by co-localization with RPA or ssDNA. Our results suggest that FANCD2 recognizes ssDNA intermediates during DNA repair and DNA damage signalling, as we observed that FANCD2 foci formation was dependent on the MRN complex and FANCD2 co-localized with ssDNA regions. To visualize ssDNA, we used a methodology that is biased towards the detection of unusually large accumulations of ssDNA. Microscopically detectable ssDNA foci may indicate the aggregation of many gapped DNA molecules within distinct nuclear micro-domains, and/or the presence of extended and irreparable ssDNA regions that constitute a sustained signal for the recruitment of caretaker proteins such as RPA, RAD51 and FANCD2. Thus, our data consolidate the idea that FANCD2 has an early function in DSB repair. As FANCD2 also bound Holliday junctions, we do not exclude the possibility that FANCD2 might also have functions at later stages of repair during Holliday junction migration and resolution.

An important molecular readout of the FA pathway is the monoubiquination of FANCD2, which is necessary for chromatin binding. DNA binding was observed with purified FANCD2 in an unmodified form. Our results are supported by cell fractionation studies, which show unmodified FANCD2 in the chromatin fraction P2 (Supplementary Figure 4). Using Xenopus extracts, it was also shown that unmodified FANCD2 associates with various DNA structures including ssDNA, dsDNA, Y-DNA and Holliday junctions (Sobeck *et al*, 2007). In the light of these results, we favour the hypothesis that monoubiquitination does not provide DNA-binding ability, but rather enhances FANCD2 binding to chromatin and facilitate protein–protein interactions. Monoubiquitination of FANCD2 may provoke a conformational change, therefore, revealing a chromatin-binding motif (Montes de Oca *et al*, 2005) to assist DNA repair and error-prone translesion synthesis. Consistent with this observation, γ-H2AX is important for the recruitment of FANCD2 into foci (Bogliolo *et al*, 2007).

MRN controls FANCD2 localization to DNA damage sites

Although MRN regulates FANCD2 foci formation in undamaged, or etoposide-treated cells, we propose that the MRN-dependent FANCD2 regulation is mostly important only in the context of replication fork collapse. Several data implicate the MRN complex in recovery from DNA replication fork collapse. It has been shown that Xenopus Mre11 is required for the restart of collapsed replication forks and ATM and ATR induce MRN complex redistribution to restarting forks (Trenz *et al*, 2006). Moreover, chromatin binding by human MRE11 is enhanced by replication fork stalling (Mirzoeva and Petrini, 2003). Most likely, these functions are necessary in the context of ICL repair, as ICL lesions create DSBs, but only after passage through S phase (Rothfuss and Grompe, 2004). After DNA DSB, a 5′-3′ exonucleolytic activity, mediated by MRN and CtIP (Sartori *et al*, 2007), generates 3′ ssDNA tails. These tails serve as probes for homologous recombination proteins identifying homologous DNA, and to initiate D-loop formation and end invasion. Using ChIP analysis, we observed FANCD2 bound to a unique DSB at 0.3 kb from the break, which might represent MRN engaged in DNA resection. We observed that binding of FANCD2 to MRE11, or the ssDNA produced by MRE11, does not inhibit MRE11 exonuclease activity. Rather, we propose that the nuclease activity of MRE11 is required for FANCD2-binding DNA lesions. This was particularly evident when we used Mirin, an inhibitor of MRN. The reduction in FANCD2 foci formation cannot be attributable to phosphorylation on serine 222 as FANCD2-S222 displays a normal level of FANCD2 foci formation after irradiation (Taniguchi *et al*, 2002b). Mirin prevents MRN-dependent activation of ATM without affecting ATM protein kinase activity, and it inhibits Mre11-associated nuclease activity (Dupre *et al*, 2008). Hence, we propose that the reduction of FANCD2 foci formation is related to the inability of MRN, a component of the ATR pathway, to

process DNA ends. Hence, MRN relay signals to the ATR pathway for monoubiquitination of FANCD2. Indeed, we observed that wortmannin, at a concentration that inhibited ATR and phosphorylation of Chk1 (Andreassen *et al*, 2004), leads to a decrease in FANCD2 foci formation in a similar fashion as Mirin-treated cells (Supplementary Figure 5). Mirin did not completely inhibit FANCD2 foci formation, suggesting that different proteins (including MRN) are implicated in the recruitment of FANCD2 on chromatin.

As the level of homology-directed repair in FA patient-derived cell line is mild (Nakanishi *et al*, 2005), we do not think that FANCD2 is essential for repair by homologous recombination. We propose that MRN and FANCD2 proteins have a crucial function in the detection/repair of a particular subset of DNA lesions, which are related to replication fork collapse (Figure 7D). MRN has a dual role in this process, it regulates not only FANCD2 protein stability, but also its accumulation to ssDNA. DNA replication of damaged DNA leads to replication fork collapse and DSB formation. MRN resect DSBs to create ssDNA, which is bound by RPA. The DNA damage response might be facilitated by binding of FANCD2 to ssDNA. In turn, RPA recruits ATR-ATRIP-HCLK2, FANCM/FAAP24 and the core complex (Collis *et al*, 2008) important for FA pathway activation. This process leads to monoubiquitination of FANCD2 and facilitates the accumulation of FANCD2 at DNA damage sites. Then, DNA repair by homologous recombination or translesion synthesis ensures that collapsed replication forks are accurately repaired to prevent genome instability.

Collectively, the experiments shown here provide a framework for future studies on the roles of the MRN nuclease in activating FANCD2 function and provide the first biochemical insight into how the MRN pathway controls FANCD2 stability and localization to DNA damage sites.

Materials and methods

Cell culture, cell synchronization, and FACS analysis

Experimental procedures are described in Supplementary data.

RNA interference

siRNAs were synthesized by Dharmacon and directed against the following target sequences: a scrambled siRNA sequence as a negative control (GACGTCATATACCAAGCTAGTTT), MRE11 (TGGC TAATGACTCTGATGATA), RAD50 (CTGCGACTTGCTCCAGATAAA), NBS1 (AACATACGTAGCTGACACAGA), FANCD2 (AACAGCCATGGA TACACTTGA) or RPA (cactctatcctctttcatg). Transfection of siRNAs was performed using oligofectamine (Invitrogen), according to the manufacturer's protocol with minor modifications. In brief, cells were seeded in six-well plates at 1.5×10^5 cells/cm^2, 16 h before transfection. For each transfection, 6 μl oligofectamine was diluted with 24 μl serum-free Opti-MEM (Invitrogen), kept at room temperature (RT) for 5 min and mixed with 360 μl serum-free Opti-MEM containing 5 μl of 100 μM oligonucleotide. The mixture was then incubated at RT for 30 min and added dropwise to the cells containing 1.6 ml serum-free Opti-MEM. Four hours after transfection, 500 μl of DMEM-FCS (30%) was added to each well. Cells were fixed or harvested 24–48–72 h after transfection, as indicated.

Immunofluorescence and laser-induced DNA DSBs

I-SceI-transfected cells were fixed 24 h post-transfection and immunofluorescence was performed as described (Rodrigue *et al*, 2006). SiRNA-transfected cells grown on coverslips were fixed 48 h post-transfection with 3.0% paraformaldehyde in PBS1X for 15 min at RT. Next, cells were permeabilized with PBS1X containing 0.3% Triton X-100 for 10 min and washed once with PBS1X. Cells were then blocked in PBS1X-NP40 (0.1%) containing 10% goat serum for 1 h and incubated in the primary antibody diluted in blocking solution for 1 h at RT. Coverslips were washed three times for 10 min with PBS1X-NP40 (0.1%) before a 1-h incubation with the appropriate secondary antibody conjugated to a fluorophore. Cells were rinsed again three times for 10 min with PBS1X-NP40 (0.1%). Coverslips were mounted onto slides with PBS1X-glycerol (90%) containing 1 mg/ml paraphenylenediamine and 0.2 μg/ml of 4′,6′-diamidino-2-phenylindole (DAPI). For the nuclear extraction protocol, cells were incubated with PBS1X-NP40 (0.5%) 10 min and fixed with 3.0% paraformaldehyde in PBS1X for 15 min at RT. Next, cells were permeabilized with PBS1X-NP40 (0.5%) for 10 min and washed once with PBS1X. Laser-induced DNA DSBs were created as described earlier (Dery *et al*, 2008).

Cell synchronization and labelling with halogenated nucleotides

Cells were synchronized with nocodazole (0.17 mM for 6 h) and mitotic shake off, collected by centrifugation (200 *g* for 10 min), plated onto 22 mm glass coverslips and incubated in fresh medium containing 1.5 mM hydroxyurea for 12 h to block cells at the G1/S boundary. To visualize replication patterns, cells were labelled for 10 min with 10 mM BrdU. To detect ssDNA foci, cells were grown for 30 h in the presence of 30 mM BrdU. To label replication patterns and ssDNA foci simultaneously, cells were grown in the presence of 30 mM CldU for 30 h, synchronized as above and labelled with 10 min pulses of IdU (10 mM).

Antibodies

The antibodies used were anti-FANCD2 rabbit antibody (Novus Biologicals), anti-FANCD2 mouse antibody (Santa Cruz), anti-MRE11 rabbit antibody (Oncogene), anti-MRE11 mouse antibody (GeneTex), anti-NBS1 and anti-RAD50 mouse antibodies (Novus Biologicals), anti-γ-H2AX mouse antibody (Upstate), anti-GAPDH (Research diagnostics), rat anti-BrdU (anti-CldU) antibody (Abcam), mouse anti-IdU antibody (Caltag Laboratories), mouse anti-RPA antibody (Calbiochem), rabbit anti-RAD51 (Santa Cruz Biotechnology) and anti-FANCI (Bethyl). Secondary antibodies for immunofluorescence used were anti-mouse and anti-rabbit antibodies conjugated with either Alexa-Fluor 488, Alexa-Fluor 555 (Molecular Probes) or Cy3-conjugated anti-rat antibodies (Jackson Immuno Research).

Cell fractionation and western blot analysis

Cell fractionation was performed as published (Zou *et al*, 2002). Cells were harvested and soluble protein extracts were prepared as described earlier (Rodrigue *et al*, 2006), resolved on 6–15% SDS–PAGE gels and blotted onto nitrocellulose (Perkin-Elmer). After transfer, the membranes were blocked for 1 h in 5% skim milk/PBS1X-Tween (0.05%) and probed overnight at 4°C with antibody as indicated. The primary monoclonal and polyclonal antibodies were diluted in 5% skim milk or 5% BSA in PBS1X-Tween (0.05%), respectively. Blotted proteins were revealed using enhanced chemiluminescence (Perkin-Elmer) after a 1-h incubation with horseradish peroxidase-conjugated anti-mouse or anti-rabbit immunoglobulins (Jackson Immunoresearch).

Co-immunoprecipitation

To study the interaction between FANCD2 and the MRN complex, FANC2-complemented PD20 cells were collected and resuspended in lysis buffer (50 mM Tris–HCl, pH 7.5, 150 mM NaCl, 0.5% NP-40) containing protease and phosphatase inhibitors (PMSF (1 mM), aprotinin (0.019 TIU/ml), leupeptin (1 μg/ml), NaF (5 mM) and Na3VO4 (1 mM)). Cells were then incubated for 30 min on ice and lysed by sonication. Insoluble material was removed by high-speed centrifugation and each immunoprecipitation was carried out using soluble protein extract (3 mg) in 1 ml lysis buffer. The samples were first incubated for 1.5 h at 4°C with the indicated antibodies. Protein complexes were then pulled down with 20 μl of protein A/G-sepharose beads (Pierce) for an hour. Immunoprecipitates were washed four times in lysis buffer and visualized by western blotting using the indicated antibodies.

Immunoprecipitations from Sf9 cells were performed as above with the following modifications. Sf9 cells (20×10^6) were infected with MRE11, NBS1, RAD50 and/or FANCD2 baculoviruses (M.O.I. ~10) for 2 days at 27°C and stored in two aliquots at −80°C. Cells were lysed in P5 buffer (50 mM $NaHPO_4$ pH 7.0, 500 mM NaCl, 5 mM imidazole, 10% glycerol, 0.05% Triton X-100) and soluble

extracts were prepared to verify the level of expression of the proteins of interest in the first aliquot. When similar levels were achieved, the remaining cells were lysed in P5 buffer and used for immunoprecipitation and immunoblotting analysis.

Immunoprecipitations with purified FANCD2 (1 μg) and MRN (1 μg) were conducted in 100 μl of lysis buffer at 37°C for 15 min. Proteins were next incubated for 30 min at 4°C with the indicated antibodies in 500 μl of lysis buffer followed by the addition of protein A/G-sepharose beads (Pierce) for 20 min. Immunoprecipitates were washed four times in lysis buffer and visualized by western blotting using the indicated antibodies.

Gel filtration analysis

Gel filtration of whole-cell extracts of FANCD2-complemented PD20 cells or Hela nuclear extracts was determined by comparison with gel filtration standards (250 μg; bovine thyroglobulin (670 kDa), bovine gamma globulin (158 kDa), chicken ovalbumin (44 kDa), horse myoglobin (17 kDa) and vitamin B-12 (1.35 kDa)). Proteins were analysed on an FPLC Explorer 10 system fitted with a 24-ml Superdex 200 PC 3.2/30 column (Pharmacia) equilibrated in R150 buffer (20 mM Tris–HCl pH 8.0, 150 mM NaCl, 10% glycerol, 1 mM EDTA, 0.5 mM DTT). Fractions (500 μl) were collected and analysed by western blotting with the indicated antibodies.

Purification of FANCD2 and MRN–FANCD2 co-complex

FANCD2 was purified using two different protocols to validate our results. The full-length *FANCD2* cDNA, containing exon 44 sequence at the 3′ end (Montes de Oca *et al*, 2005), was amplified by PCR and cloned in pET52b (Novagen). The insert, along with 3′-Strep-tag and 5′-His-tag, was cloned in pFASTBAC1. Recombinant baculoviruses were produced and used to infect 400 ml of Sf9 insect cells (multiplicity of infection = 10) for 2 days at 27°C. The cell pellet was resuspended in 50 ml of P5 buffer containing 5 mM imidazole and the protease inhibitors PMSF (1 mM), aprotinin (0.019 TIU/ml) and leupeptin (1 μg/ml). The suspension was lysed using a Dounce homogenizer (10 strokes), sonicated four times for 30 s, and then homogenized a second time. Insoluble material was removed by centrifugation (twice at 35 000 r.p.m. for 1 h in a Sorvall Ultra Pro 80 T647.5 rotor). The supernatant was loaded on a 5-ml Talon column (Clontech) and washed stepwise with P buffer containing 30 mM (75 ml), and 50 mM (25 ml) imidazole. The FANCD2 protein was then eluted with a 40-ml linear gradient of 0.05–1.0 M imidazole in P buffer. The proteins were identified by SDS–PAGE, pooled and dialysed against ST buffer (50 mM $NaPO_4$ pH 7.5, 150 mM NaCl, 10% glycerol, 1 mM DTT) and loaded on a 1-ml Streptactin (Novagen) and processed according to the manufacturer's instructions. Individual fractions containing FANCD2 were dialysed for 90 min in three successive steps in D buffer (20 mM Tris–HCl pH 8, 10% glycerol, 1 mM DTT, 0.05% Tween 20) containing 500, 250 and 100 mM NaCl. The fractions were concentrated using an Amicon ultra-15 column (Millipore) and stored in aliquots at −80°C.

The full-length *FANCD2* cDNA, containing exon 44 sequence at the 3′ end (Montes de Oca *et al*, 2005), was sub-cloned into pFastBac1 (Invitrogen) using standard procedures. The encoded FANCD2 protein comprised a Flag epitope (MDYKDDDDK), and a linker of two amino acids (EF), preceding its starting methionine. Recombinant baculoviruses were produced and used to infect Sf21 insect cells, according to instructions from Invitrogen. FANCD2 was purified from two 500 ml cultures of Sf21 cells (1.5×10^6 cells/ml) infected with Flag-FANCD2 baculoviruses at 27°C for 48 h. Cells were spun down and resuspended in four-packed cell volume of buffer A (50 mM Tris–HCl pH 7.2, 0.15 M NaCl, 10% glycerol, 0.02% Triton X-100, 1 mM EDTA and 1 mM DTT) containing protease and phosphatase inhibitors. The cell suspension was lysed using a Dounce homogenizer and sonicated three times for 30 s. Insoluble material was spun down for 90 min at 100 000 *g*. The cleared lysate was loaded onto two connected 5 cm^3 HiTrap Heparin HP columns (Amersham Pharmacia), washed with 50 ml of buffer A and fractionated with a 100-ml gradient to 1 M NaCl. Fractions containing FANCD2 were pooled and loaded directly onto a 1-cm^3 ANTI-FLAG M2 affinity gel (Sigma) equilibrated in buffer A. The column was washed with 5 ml of buffer A supplemented with 100 mM arginine. FANCD2 was eluted with 5 ml of buffer A supplemented with 100 mg/ml of × 3 FLAG peptide (SIGMA). Homogeneous FANCD2 fractions were pooled, concentrated four-folds on a Vivaspin 2 spin column (100 000 MWCO, VIVASCIENCE), dialysed against buffer A and stored in aliquots at −80°C.

For the purification of MRN–FANCD2 co-complex, spinner flasks (450 ml) of Sf9 cells (1×10^6 cells/ml) were infected with the MRE11, RAD50, NBS1 and FANCD2 baculoviruses (M.O.I = 10 for the His-tagged viruses and M.O.I. = 20 for untagged viruses) for 2 days at 27°C. Cells were harvested, frozen in dry ice/ethanol and stored at −20°C. Nickel chromatography and Q-sepharose were performed essentially as described (Lee and Paull, 2006).

DNA-binding assays and exonuclease assays

Reactions (10 μl) contained ^{32}P-labelled DNA oligonucleotides and FANCD2, at the indicated concentrations, in MOPS buffer (25 mM MOPS at pH 7.0, 60 mM KCl, 0.2% Tween 20, 2 mM DTT and 5 mM $MnCl_2$). Reaction mixtures were incubated at 37°C for 15 min followed by 10 min of fixation in 0.2% glutaraldehyde. Reactions with ∅X174 DNA substrates were performed in buffer B (25 mM Tris–HCl pH 7.2, 75 mM NaCl, 5% glycerol, 0.01% Triton X-100, 0.5 mM EDTA and 0.5 mM DTT). Reaction mixtures were incubated at RT for 30 min. FANCD2–DNA complexes were resolved by electrophoresis through 0.8% agarose gels, run at 4.5 V/cm for 4 h, in TAE buffer, at RT. ^{32}P-labelled DNA was visualized by autoradiography. DNA substrates used in exonuclease assays were generated with purified oligonucleotides as described (Lee *et al*, 2003). Exonuclease reactions were performed as described earlier (Boisvert *et al*, 2005).

Electron microscopy

Reactions with gapped DNA substrates were performed in buffer B (25 mM Tris–HCl pH 7.2, 75 mM NaCl, 5% glycerol, 0.01% Triton X-100, 0.5 mM EDTA and 0.5 mM DTT). Reaction mixtures were incubated at RT for 30 min, diluted and washed in 5 mM magnesium acetate and then stained with 2% uranyl acetate as described (Sogo *et al*, 1987). Protein–DNA complexes were visualized using a Phillips CM100 electron microscope.

Chromatin immunoprecipitations

Chromatin Immunoprecipitations were performed as described by Rodrigue *et al* (2006).

Supplementary data

Supplementary data are available at *The EMBO Journal* Online (http://www.embojournal.org).

Acknowledgements

We are grateful to Fanconi Anemia Research Fund, Hans Joenje, Johan P de Winter, Shobbir Hussain, Markus Grompe, Yossi Shiloh for providing cell lines, Unité d'Imagerie Cellulaire (CRHDQ) for technical help, Nancy Roberge for FACS analysis, and Eric Paquet for statistical analyses. We thank Geneviève Almouzni for experimental advices, Marine Rentler Courdier for the complementation of FA-A cells and Steve West and Tom Moss for critical reading of the paper. We are indebted to Nathalie Garin and Marcel Allegrini for their assistance with confocal microscopy. AR, IB and JV are recipient of a CIHR doctoral scholarship, a Fanconi anemia-CIHR post-doctoral fellowship and FQRNT fellowship, respectively. This work was supported by funds from the Swiss National Science Foundation, grant 3100A0-100135 and PP00A-102891 (AC) and grant 3100A0-103962 (AS), by the Novartis Foundation (SG) and from the National Cancer Institute of Canada (grant # 017121 to JYM).

References

Akkari YM, Bateman RL, Reifsteck CA, Olson SB, Grompe M (2000) DNA replication is required to elicit cellular responses to psoralen-induced DNA interstrand cross-links. *Mol Cell Biol* **20:** 8283–8289

Andreassen PR, D'Andrea AD, Taniguchi T (2004) ATR couples FANCD2 monoubiquitination to the DNA-damage response. *Genes Dev* **18:** 1958–1963

Auerbach AD, Wolman SR (1976) Susceptibility of Fanconi's anaemia fibroblasts to chromosome damage by carcinogens. *Nature* **261:** 494–496

Becker E, Meyer V, Madaoui H, Guerois R (2006) Detection of a tandem BRCT in Nbs1 and Xrs2 with functional implications in the DNA damage response. *Bioinformatics* **22:** 1289–1292

Bogliolo M, Lyakhovich A, Callen E, Castella M, Cappelli E, Ramirez MJ, Creus A, Marcos R, Kalb R, Neveling K, Schindler D, Surralles J (2007) Histone H2AX and Fanconi anemia FANCD2 function in the same pathway to maintain chromosome stability. *EMBO J* **26:** 1340–1351

Boisvert FM, Dery U, Masson JY, Richard S (2005) Arginine methylation of MRE11 by PRMT1 is required for DNA damage checkpoint control. *Genes Dev* **19:** 671–676

Bridge WL, Vandenberg CJ, Franklin RJ, Hiom K (2005) The BRIP1 helicase functions independently of BRCA1 in the Fanconi anemia pathway for DNA crosslink repair. *Nat Genet* **37:** 953–957

Collis SJ, Ciccia A, Deans AJ, Horejsi Z, Martin JS, Maslen SL, Skehel JM, Elledge SJ, West SC, Boulton SJ (2008) FANCM and FAAP24 function in ATR-mediated checkpoint signaling independently of the fanconi anemia core complex. *Mol Cell* **32:** 313–324

De Silva IU, McHugh PJ, Clingen PH, Hartley JA (2000) Defining the roles of nucleotide excision repair and recombination in the repair of DNA interstrand cross-links in mammalian cells. *Mol Cell Biol* **20:** 7980–7990

Dery U, Coulombe Y, Rodrigue A, Stasiak A, Richard S, Masson JY (2008) A glycine-arginine domain in control of the human MRE11 DNA repair protein. *Mol Cell Biol* **28:** 3058–3069

Dery U, Masson JY (2007) Twists and turns in the function of DNA damage signaling and repair proteins by post-translational modifications. *DNA Repair (Amst)* **6:** 561–577

Dupre A, Boyer-Chatenet L, Sattler RM, Modi AP, Lee JH, Nicolette ML, Kopelovich L, Jasin M, Baer R, Paull TT, Gautier J (2008) A forward chemical genetic screen reveals an inhibitor of the Mre11-Rad50-Nbs1 complex. *Nat Chem Biol* **4:** 119–125

Garcia-Higuera I, Taniguchi T, Ganesan S, Meyn MS, Timmers C, Hejna J, Grompe M, D'Andrea AD (2001) Interaction of the Fanconi anemia proteins and BRCA1 in a common pathway. *Mol Cell* **7:** 249–262

Godthelp BC, Wiegant WW, van Duijn-Goedhart A, Scharer OD, van Buul PP, Kanaar R, Zdzienicka MZ (2002) Mammalian Rad51C contributes to DNA cross-link resistance, sister chromatid cohesion and genomic stability. *Nucleic Acids Res* **30:** 2172–2182

Grompe M, D'Andrea A (2001) Fanconi anemia and DNA repair. *Hum Mol Genet* **10:** 2253–2259

Gurtan AM, Stuckert P, D'Andrea AD (2006) The WD40 repeats of FANCL are required for Fanconi anemia core complex assembly. *J Biol Chem* **281:** 10896–10905

Hall SD, Kane MF, Kolodner RD (1993) Identification and characterization of the Escherichia coli RecT protein, a protein encoded by the recE region that promotes renaturation of homologous single-stranded DNA. *J Bacteriol* **175:** 277–287

Howlett NG, Taniguchi T, Olson S, Cox B, Waisfisz Q, De Die-Smulders C, Persky N, Grompe M, Joenje H, Pals G, Ikeda H, Fox EA, D'Andrea AD (2002) Biallelic inactivation of BRCA2 in Fanconi anemia. *Science* **297:** 606–609

Ishiai M, Kitao H, Smogorzewska A, Tomida J, Kinomura A, Uchida E, Saberi A, Kinoshita E, Kinoshita-Kikuta E, Koike T, Tashiro S, Elledge SJ, Takata M (2008) FANCI phosphorylation functions as a molecular switch to turn on the Fanconi anemia pathway. *Nat Struct Mol Biol* **15:** 1138–1146

Jazayeri A, Falck J, Lukas C, Bartek J, Smith GC, Lukas J, Jackson SP (2006) ATM- and cell cycle-dependent regulation of ATR in response to DNA double-strand breaks. *Nat Cell Biol* **8:** 37–45

Kim YC, Koh JT, Shin BA, Ahn KY, Choi BK, Kim CG, Kim KK (2002) An antisense construct of full-length human RAD50 cDNA confers sensitivity to ionizing radiation and alkylating agents on human cell lines. *Radiat Res* **157:** 19–25

Lee JH, Ghirlando R, Bhaskara V, Hoffmeyer MR, Gu J, Paull TT (2003) Regulation of Mre11/Rad50 by Nbs1: effects on nucleotide-dependent DNA binding and association with ataxia-telangiectasia-like disorder mutant complexes. *J Biol Chem* **278:** 45171–45181

Lee JH, Paull TT (2006) Purification and biochemical characterization of ataxia-telangiectasia mutated and Mre11/Rad50/Nbs1. *Methods Enzymol* **408:** 529–539

Levitus M, Waisfisz Q, Godthelp BC, de Vries Y, Hussain S, Wiegant WW, Elghalbzouri-Maghrani E, Steltenpool J, Rooimans MA, Pals G, Arwert F, Mathew CG, Zdzienicka MZ, Hiom K, De Winter JP, Joenje H (2005) The DNA helicase BRIP1 is defective in Fanconi anemia complementation group J. *Nat Genet* **37:** 934–935

Lim DS, Kim ST, Xu B, Maser RS, Lin JY, Petrini JHJ, Kastan MB (2000) ATM phosphorylates p95/nbs1 in an S-phase checkpoint pathway. *Nature* **404:** 613–617

McHugh PJ, Sones WR, Hartley JA (2000) Repair of intermediate structures produced at DNA interstrand crosslinks in S. cerevisiae. *Mol Cell Biol* **20:** 3425–3433

Meetei AR, Yan Z, Wang W (2004) FANCL replaces BRCA1 as the likely ubiquitin ligase responsible for FANCD2 monoubiquitination. *Cell Cycle* **3:** 179–181

Mirzoeva OK, Petrini JH (2003) DNA replication-dependent nuclear dynamics of the Mre11 complex. *Mol Cancer Res* **1:** 207–218

Montes de Oca R, Andreassen PR, Margossian SP, Gregory RC, Taniguchi T, Wang X, Houghtaling S, Grompe M, D'Andrea AD (2005) Regulated interaction of the Fanconi anemia protein, FANCD2, with chromatin. *Blood* **105:** 1003–1009

Moreno-Herrero F, de Jager M, Dekker NH, Kanaar R, Wyman C, Dekker C (2005) Mesoscale conformational changes in the DNA-repair complex Rad50/Mre11/Nbs1 upon binding DNA. *Nature* **437:** 440–443

Nakanishi K, Taniguchi T, Ranganathan V, New HV, Moreau LA, Stotsky M, Mathew CG, Kastan MB, Weaver DT, D'Andrea AD (2002) Interaction of FANCD2 and NBS1 in the DNA damage response. *Nat Cell Biol* **4:** 913–920

Nakanishi K, Yang YG, Pierce AJ, Taniguchi T, Digweed M, D'Andrea AD, Wang ZQ, Jasin M (2005) Human Fanconi anemia monoubiquitination pathway promotes homologous DNA repair. *Proc Natl Acad Sci USA* **102:** 1110–1115

Niedernhofer LJ, Lalai AS, Hoeijmakers JH (2005) Fanconi anemia (cross)linked to DNA repair. *Cell* **123:** 1191–1198

Park WH, Margossian S, Horwitz AA, Simons AM, D'Andrea AD, Parvin JD (2005) Direct DNA binding activity of the Fanconi anemia D2 protein. *J Biol Chem* **280:** 23593–23598

Paull TT, Gellert M (1998) The 3′-exonuclease to 5′-exonuclease activity of Mre11 facilitates repair of DNA double-strand breaks. *Mol Cell* **1:** 969–979

Pichierri P, Averbeck D, Rosselli F (2002) DNA cross-link-dependent RAD50/MRE11/NBS1 subnuclear assembly requires the Fanconi anemia C protein. *Hum Mol Genet* **11:** 2531–2546

Pichierri P, Rosselli F (2004) The DNA crosslink-induced S-phase checkpoint depends on ATR-CHK1 and ATR-NBS1-FANCD2 pathways. *EMBO J* **23:** 1178–1187

Pierce AJ, Johnson RD, Thompson LH, Jasin M (1999) XRCC3 promotes homology-directed repair of DNA damage in mammalian cells. *Genes Dev* **13:** 2633–2638

Raderschall E, Golub EI, Haaf T (1999) Nuclear foci of mammalian recombination proteins are located at single-stranded DNA regions formed after DNA damage. *Proc Natl Acad Sci USA* **96:** 1921–1926

Raschle M, Knipsheer P, Enoiu M, Angelov T, Sun J, Griffith JD, Ellenberger TE, Scharer OD, Walter JC (2008) Mechanism of replication-coupled DNA interstrand crosslink repair. *Cell* **134:** 969–980

Reid S, Schindler D, Hanenberg H, Barker K, Hanks S, Kalb R, Neveling K, Kelly P, Seal S, Freund M, Wurm M, Batish SD, Lach FP, Yetgin S, Neitzel H, Ariffin H, Tischkowitz M, Mathew CG, Auerbach AD, Rahman N (2007) Biallelic mutations in PALB2 cause Fanconi anemia subtype FA-N and predispose to childhood cancer. *Nat Genet* **39:** 162–164

Ridpath JR, Nakamura A, Tano K, Luke AM, Sonoda E, Arakawa H, Buerstedde JM, Gillespie DA, Sale JE, Yamazoe M, Bishop DK, Takata M, Takeda S, Watanabe M, Swenberg JA, Nakamura J (2007) Cells deficient in the FANC/BRCA pathway are hypersensitive to plasma levels of formaldehyde. *Cancer Res* **67:** 11117–11122

Rodrigue A, Lafrance M, Gauthier M-C, McDonald D, Hendzel M, West SC, Jasin M, Masson JY (2006) Interplay between human DNA repair proteins at a unique double-strand breaks *in vivo*. *EMBO J* **25:** 222–231

Rothfuss A, Grompe M (2004) Repair kinetics of genomic interstrand DNA cross-links: evidence for DNA double-strand break-

dependent activation of the Fanconi anemia/BRCA pathway. *Mol Cell Biol* **24:** 123–134

Sartori AA, Lukas C, Coates J, Mistrik M, Fu S, Bartek J, Baer R, Lukas J, Jackson SP (2007) Human CtIP promotes DNA end resection. *Nature* **450:** 509–514

Sims AE, Spiteri E, Sims III RJ, Arita AG, Lach FP, Landers T, Wurm M, Freund M, Neveling K, Hanenberg H, Auerbach AD, Huang TT (2007) FANCI is a second monoubiquitinated member of the Fanconi anemia pathway. *Nat Struct Mol Biol* **14:** 564–567

Smogorzewska A, Matsuoka S, Vinciguerra P, McDonald III ER, Hurov KE, Luo J, Ballif BA, Gygi SP, Hofmann K, D'Andrea AD, Elledge SJ (2007) Identification of the FANCI protein, a monoubiquitinated FANCD2 paralog required for DNA repair. *Cell* **129:** 289–301

Sobeck A, Stone S, Hoatlin ME (2007) DNA structure-induced recruitment and activation of the Fanconi anemia pathway protein FANCD2. *Mol Cell Biol* **27:** 4283–4292

Sogo J, Stasiak A, De Bernadin W, Losa R, Koller T (1987) Binding of proteins to nucleic acids as studied by electron microscopy. In *Electron Microscopy in Molecular Biology*, Sommerville J, Scheer U (eds), pp 61–79. Oxford: IRL Press

Stewart GS, Maser RS, Stankovic T, Bressan DA, Kaplan MI, Jaspers NGJ, Raams A, Byrd PJ, Petrini JHJ, Taylor AMR (1999) The DNA double-strand break repair gene hMRE11 is mutated in individuals with an Ataxia telangiectasia-like disorder. *Cell* **99:** 577–587

Taniguchi T, Garcia-Higuera I, Andreassen PR, Gregory RC, Grompe M, D'Andrea AD (2002a) S-phase-specific interaction of the Fanconi anemia protein, FANCD2, with BRCA1 and RAD51. *Blood* **100:** 2414–2420

Taniguchi T, Garcia-Higuera I, Xu B, Andreassen PR, Gregory RC, Kim ST, Lane WS, Kastan MB, D'Andrea AD (2002b) Convergence of the fanconi anemia and ataxia telangiectasia signaling pathways. *Cell* **109:** 459–472

Thresher RJ, Makhov AM, Hall SD, Kolodner R, Griffith JD (1995) Electron microscopic visualization of RecT protein and its complexes with DNA. *J Mol Biol* **254:** 364–371

Timmers C, Taniguchi T, Hejna J, Reifsteck C, Lucas L, Bruun D, Thayer M, Cox B, Olson S, D'Andrea AD, Moses R, Grompe M (2001) Positional cloning of a novel fanconi anemia gene, FANCD2. *Mol Cell* **7:** 241–248

Trenz K, Smith E, Smith S, Costanzo V (2006) ATM and ATR promote Mre11 dependent restart of collapsed replication forks and prevent accumulation of DNA breaks. *EMBO J* **25:** 1764–1774

Trujillo KM, Yuan SSF, Lee EYHP, Sung P (1998) Nuclease activities in a complex of human recombination and DNA repair factors Rad50, Mre11, and p95. *J Biol Chem* **273:** 21447–21450

Wang W (2007) Emergence of a DNA-damage response network consisting of Fanconi anaemia and BRCA proteins. *Nat Rev Genet* **8:** 735–748

Williams RS, Williams JS, Tainer JA (2007) Mre11-Rad50-Nbs1 is a keystone complex connecting DNA repair machinery, double-strand break signaling, and the chromatin template. *Biochem Cell Biol* **85:** 509–520

Xia B, Dorsman JC, Ameziane N, de Vries Y, Rooimans MA, Sheng Q, Pals G, Errami A, Gluckman E, Llera J, Wang W, Livingston DM, Joenje H, de Winter JP (2007) Fanconi anemia is associated with a defect in the BRCA2 partner PALB2. *Nat Genet* **39:** 159–161

Zhu W, Dutta A (2006) Activation of fanconi anemia pathway in cells with re-replicated DNA. *Cell Cycle* **5:** 2306–2309

Zhu XD, Kuster B, Mann M, Petrini JHJ, de Lange T (2000) Cell-cycle-regulated association of RAD50/MRE11/NBS1 with TRF2 and human telomeres. *Nat Genet* **25:** 347–352

Zou L, Cortez D, Elledge SJ (2002) Regulation of ATR substrate selection by Rad17-dependent loading of Rad9 complexes onto chromatin. *Genes Dev* **16:** 198–208